Supplemental Material

Supplemental Methods

Isolation of *fum2* mutants

The Col-0 T-DNA insertion lines *fum2-1* (SALK_025631) and *fum2-2* (GABI_107E05) (Pracharoenwattana et al., 2010; Brotman et al., 2011) were ordered from the Arabidopsis Biological Resource Center. The unpublished line *fum2-3* (SALK_149466) was kindly provided by Junshi Yazaki (The Salk Institute, La Jolla). Homozygous individuals for all three lines were successfully isolated by PCR-based genotyping on genomic DNA extractions using primers: *FUM2* fwd3 GGGAAGCCATAATGGAAG, *FUM2* rev5 GTCAAAGGTGTAGCATCTTGAG and Salk left border primer LBaI TGGTTCACGTAGTGGGCCATCG or GABI-LB CCCATTTGGACGTGAATGT, respectively. Sequencing of T-DNA border PCR products confirmed all three insertions in the third intron of *FUM2* locus.

dpe2 lines in WS background (Lu and Sharkey, 2004) were kindly provided by Thomas Sharkey (University of Wisconsin, Madison).

Complementation of *cpgi* mutants

The cPGI open reading frame was amplified from a leave tissue cDNA pool using primers cPGI fwd TOPO (CACCATGGCGTCATCAACCGCTTTG) and cPGI rev 2 (TCACATCTGGGGCTCGGAACTTGTC) and cloned into pENTR/D-TOPO. The sequence verified *cPGI* cDNA was transferred by LR reaction into the destination vector pAMPAT (GenBank accession number AY436765) harboring either a cauliflower mosaic virus 35S promoter (CaMV35S:pAMPAT) or the seed specific Unknown Seed Protein promoter of 637 bp described in Bäumlein et al. (1991, pUSP:pAMPAT) to drive transgene expression *in planta*. Binary vectors p35S:cPGI:pAMPAT and pUSP:cPGI:pAMPAT were transformed into *Agrobacterium tumefaciens* GV3101 pMP90 RK. For complementation with pUBQ10:cPGI the same construct used for cPGI localization described in Materials and Methods was employed (cPGI open reading frame in pHygII-UT-c-term-Venus). Complementation constructs were subsequently transformed into heterozygous *cpgi* T-DNA mutants using the floral dip method and transformed individuals identified based on the respective resistance marker

(phosphinothricin for pAMPAT, hygromycin for pHygII-UT-c-term-Venus). Primary transformants (T1) were genotyped by genomic DNA PCR for presence and allelic state of the *cpgi* T-DNA insertion.

USP promoter uidA reporter gene analyses

The uidA coding sequence of the entry vector pENTR-GUS (Life Technogies, Darmstadt, Germany) was transferred by LR reaction into pUSP:pAMPAT to yield the binary vector pUSP:uidA:pAMPAT. pUSP:uidA:pAMPAT was transformed into *Agrobacterium tumefaciens* GV3101 pMP90 RK which was subsequently used to transform *Arabidopsis thaliana* Col-0 plants using the floral dip method. Successfully transformed plants were selected based on phosphinotricin resistance and analyzed for β-glucuronidase activity as described previously (Wester et al., 2009).

Supplemental References

Brotman Y, Riewe D, Lisec J, Meyer RC, Willmitzer L, Altmann T (2011) Identification of enzymatic and regulatory genes of plant metabolism through QTL analysis in *Arabidopsis*. J Plant Physiol **168:** 1387-1394

Wester K, Digiuni S, Geier F, Timmer J, Fleck C, Hulskamp M (2009) Functional diversity of R3 single-repeat genes in trichome development. Development **136:** 1487-1496

Supplemental Tables

Supplemental Table SI: Observed and expected distribution of genotypes from the progeny of heterozygous *cPGI* T-DNA mutants. The number of expected individuals per genotype was calculated based on the expected genotype distribution taking the decreased transmission efficiency (Table I) into account as outlined in Supplemental Figure S7.

Ecotype		*cpgi*/*cpgi*	*cPGI*/*cpgi*	*cPGI*/*cPGI*	Total
cpgi-1	obs.	0	148	156	304
	exp.	18.2	112.5	173.3	304
cpgi-2	obs.	0	159	146	305
	exp.	16.5	119.6	168.9	305

Supplemental Table SII: Germination rate [%] of segregating seeds collected from heterozygous *cPGI/cpgi* plants and Col-0 wild type. Germination of 100 seeds per plate and genotype was scored as radicle emergence seven days after plates with imbibed and stratified (two days at 4°C) seeds had been transferred into long-day (16/8 h day/night) conditions. Average ± SD, n = 9.

	Col-0	*cPGI/cpgi-1*	*cPGI/cpgi-2*
Germination rate [%]	96.0 ± 1.7	98.7 ± 1.1	98.4 ± 1.7

Supplemental Figures

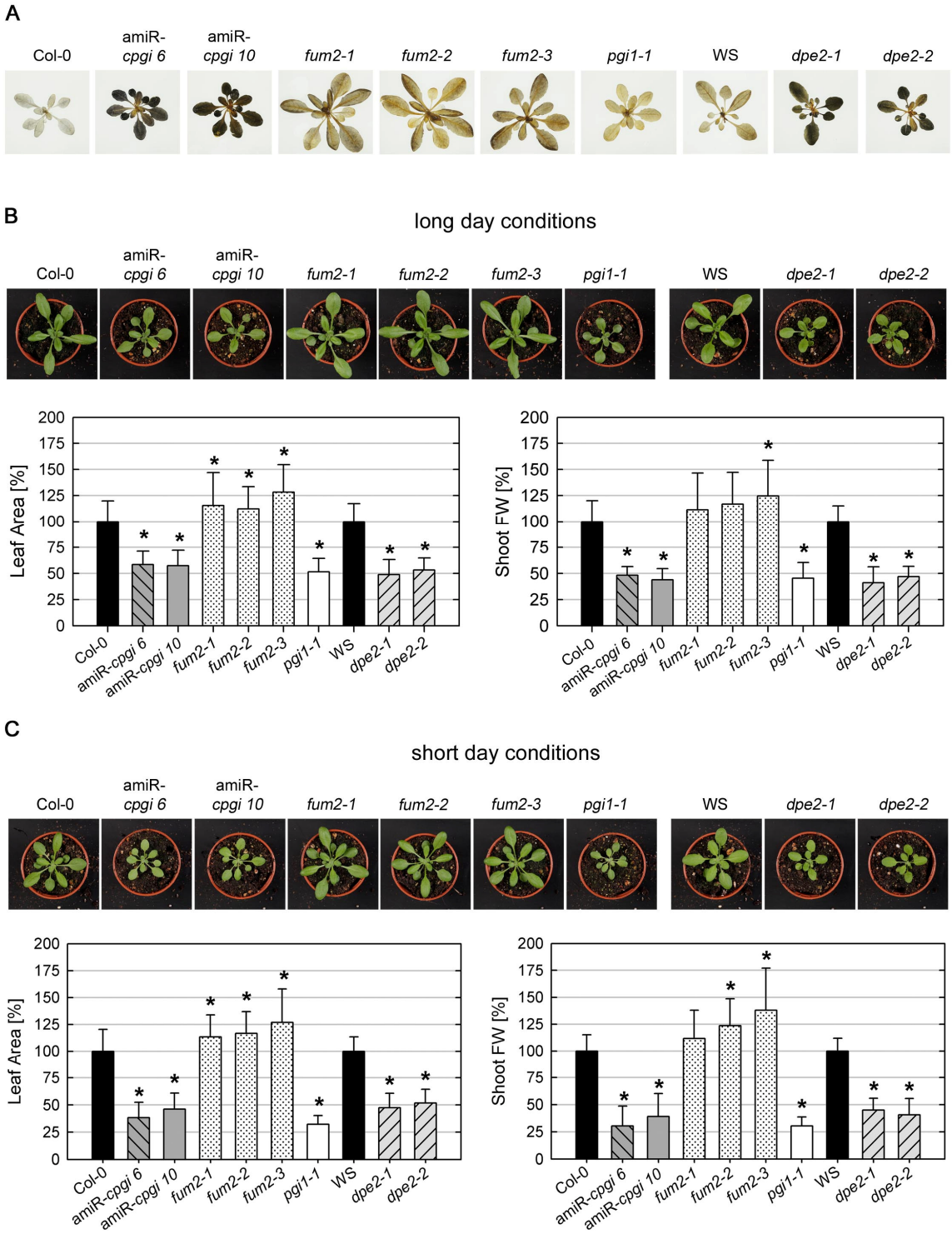

Supplemental Figure S1: Plant growth of mutants and corresponding wild types in long and short-day conditions.

A: Starch staining of whole rosettes harvested at the end of the night from long-day grown plants.
B: Representative images, leaf area and shoot fresh weight data of different plant lines normalized to wild type after growth of 21 days in long-day (16/8 h, day/night) conditions.
C: Representative images, leaf area and shoot fresh weight data of different plant lines normalized to wild type after growth of 21 days in short-day conditions (8/16 h, day/night).

Data represent averages ± SD from three independent experiments (n = 15-30). Asterisks indicate significant differences to wild type (student's t-test, $\alpha \leq 0.05$). Wassilewskija (WS) accession is the corresponding wild type for *dpe2* mutants. All other mutants are in Columbia-0 (Col-0) background. Due to general growth variation between replicate experiments data were normalized relative to wild type [%].

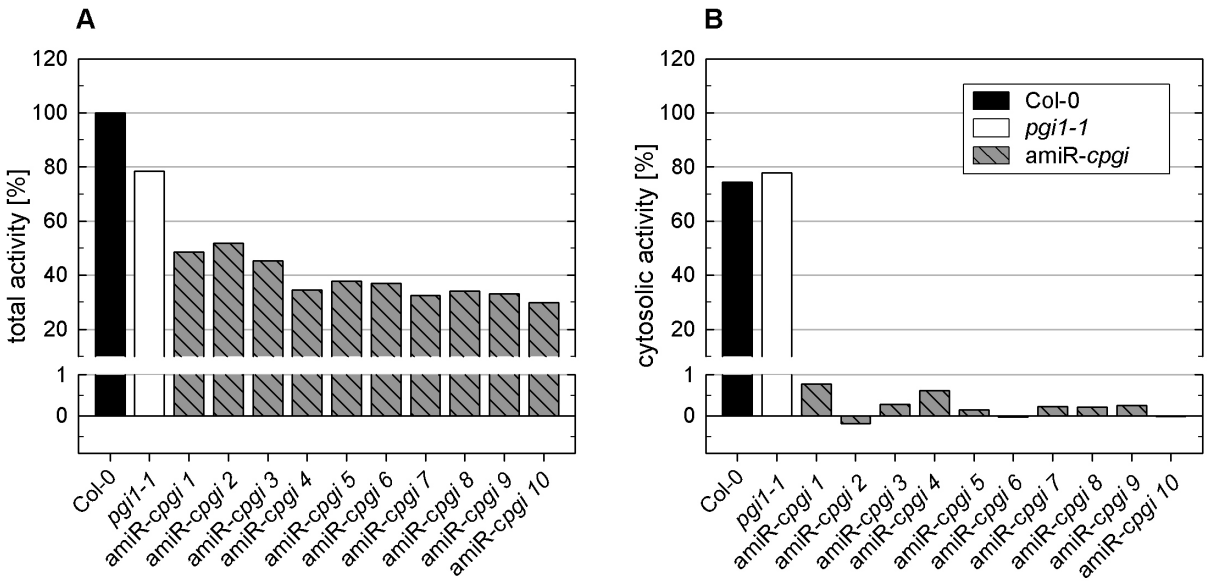

Supplemental Figure S2: Reduced PGI activity in amiR-*cpgi* plants.

Total PGI activity (A) and cytosolic PGI activity after heat inactivation of plastidic PGI (B) in leaf extracts of ten independent amiR-*cpgi* lines. Rates were normalized to total activity in leaf extracts from Col-0 wild type (100% corresponds to an activity of 0.219 nmol • (µg total protein • min)$^{-1}$). amiR-*cpgi* lines no. 6 and 10 were selected for further analysis. Note that residual activity in amiR-*cpgi* plants is less than 1% after inactivation of plastidic PGI in all lines and not detectable in amiR-*cpgi 6* and amiR-*cpgi 10* in particular.

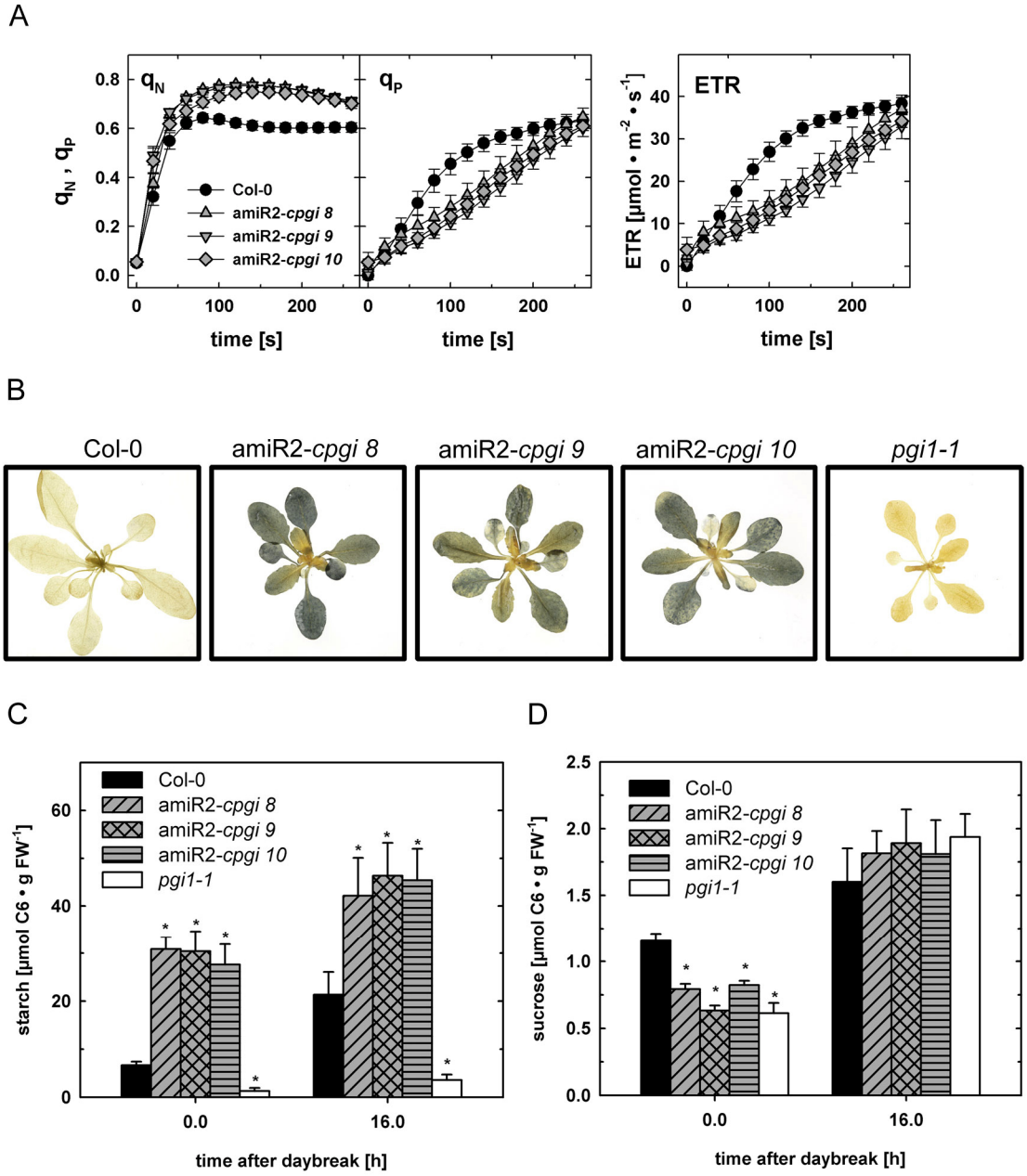

Supplemental Figure S3: Photosynthetic and metabolic data of three independent lines expressing the second amiRNA targeting *cPGI* transcript (amiR2-*cpgi*).

A: Non-photochemical (q_N) and photochemical (q_P) quench coefficients and electron transport rates (ETR) in leaves during light induction of dark adapted plants.

B: Starch staining of whole rosette leaves at the end of the night. Whole rosettes were harvested at the end of the night period and stained with potassium iodine solution. Dark leaves indicate the presence of a high starch content.

C-D: Starch and sucrose content in rosette leaves in wild-type and mutant plants at the end of the night and at the end of the day (0 h and 16 h after daybreak, respectively). Asterisks indicate significant difference compared to wild type. Average ± SEM. $n = 5$, $p \leq 0.05$.

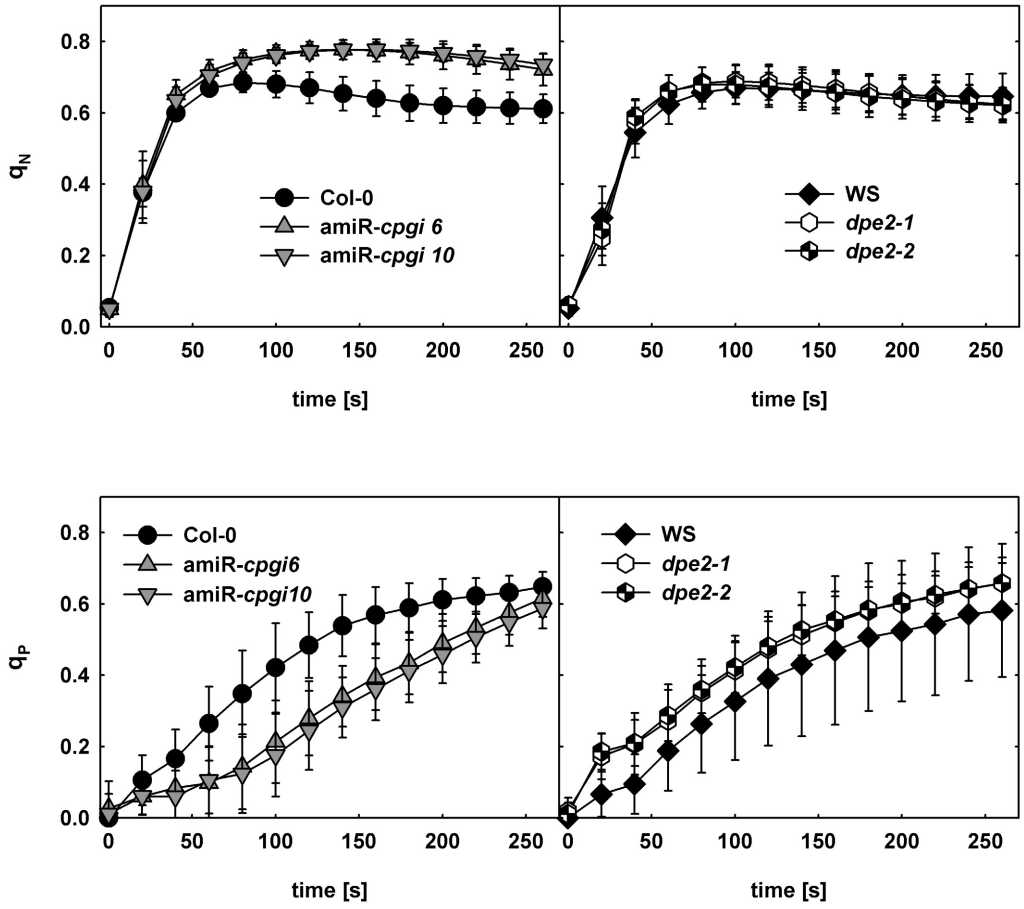

Supplemental Figure S4: Non-photochemical (q_N) and photochemical (q_P) quench coefficients during light induction curves in amiR-*cpgi* and *dpe2* mutants and corresponding wild-type plants grown in long-day conditions. Average ± SD (n = 36–60).

Supplemental Figure S5: Phenotype of a homozygous *cpgi-1* plant expressing *cPGI* under control of the CaMV35 promoter

A: Image of a flowering homozygous *cpgi-1* plant expressing *cPGI* under control of the CaMV35 promoter. Self-fertilized siliques do not elongate or contain any seeds (upper inset) while pistils pollinated with Col-0 wild-type pollen on the same plant elongate and produce seeds (lower inset). Scale bar = 5 mm.

B: Alexander-stained anther of a homozygous *cpgi-1* plant expressing *cPGI* under control of the CaMV35 promoter and of a Col-0 wild-type anther. Viable pollen grains accumulate red stain. Scale bar = 200 µm.

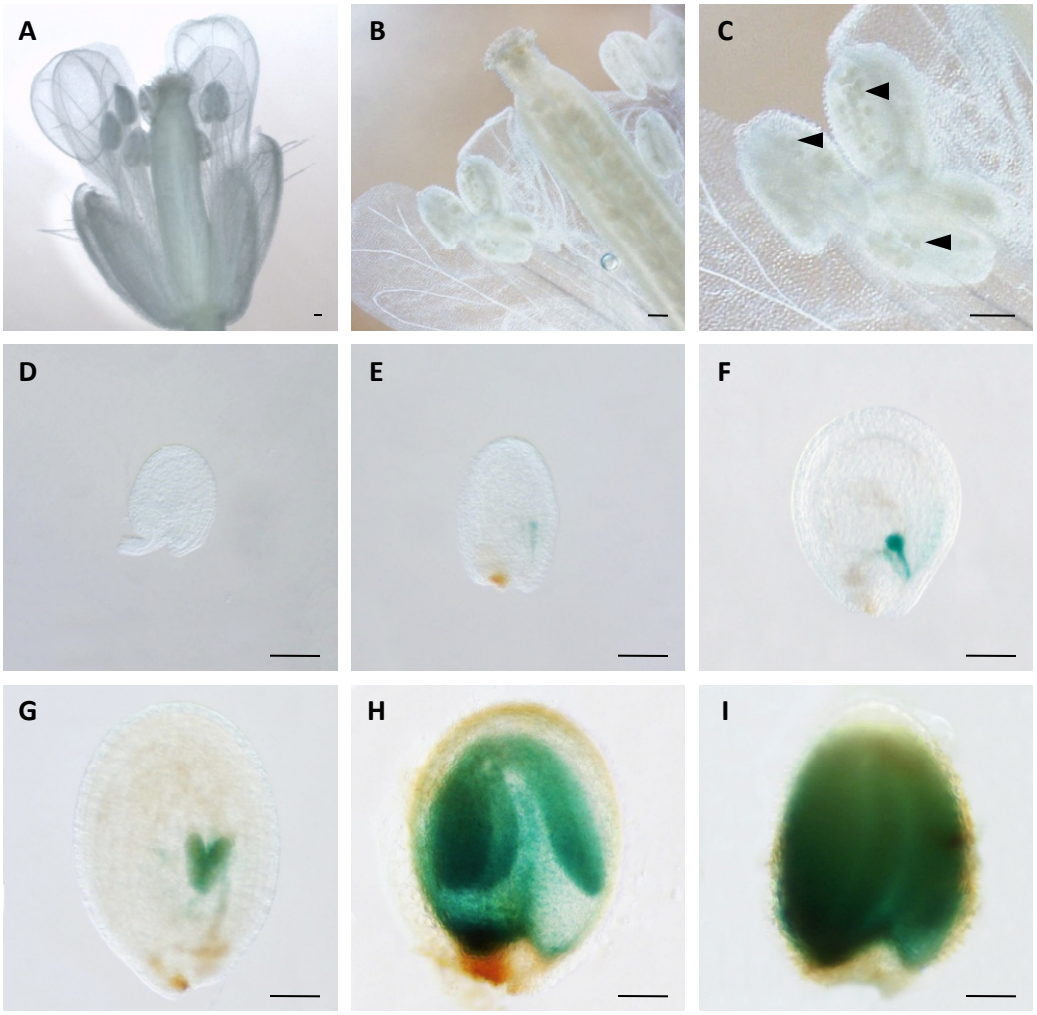

Supplemental Figure S6: USP promoter activity monitored histochemically as β-glucuronidase activity and analyzed microscopically in flowers (A-C) and developing seeds (D-I) of transgenic pUSP:uidA plants.

A: Whole flower.
B/C: Part of a flower. Arrows indicate mature pollen grains. C is a partial magnification of B
D: Seed 1 DAF.
E: Seed 3 DAF.
F: Seed 4 DAF.
G: Seed 6 DAF.
H: Seed 8 DAF.
I: Seed 12 DAF.
DAF = Days after flowering. Scale bar = 100 µm

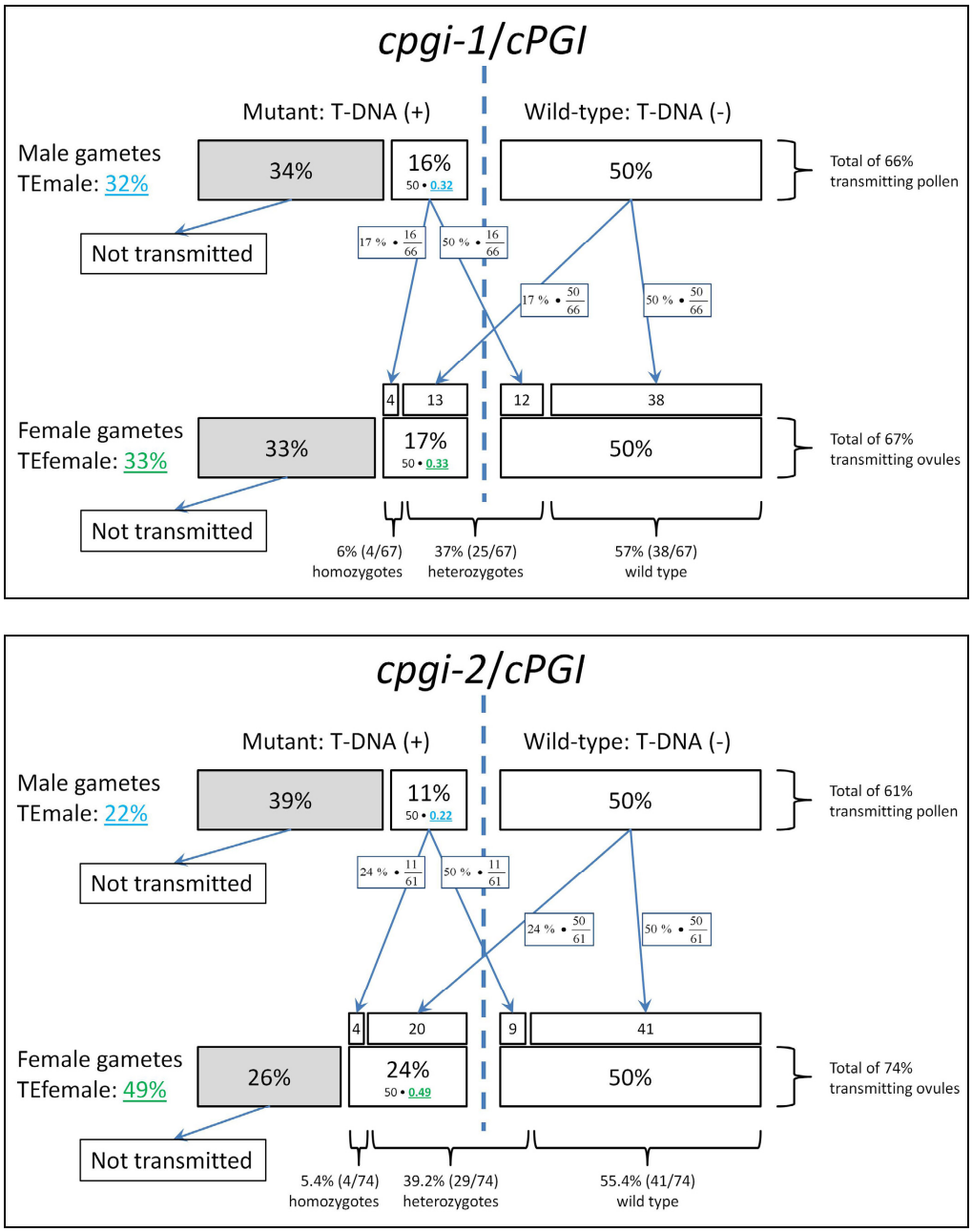

Supplemental Figure S7: Diagram illustrating the calculation of the expected genotype distribution in the self progeny of heterozygous *cPGI/cpgi* plants. The calculation takes the observed transmission efficiencies for *cpgi-1* and *cpgi-2* (Table I) into account and follows the calculation presented in Figure 4 of Howden et al. (1998). Percentages of expected genotypes are given in the bottommost line of each graph.